
Senescence and tumor clearance triggered by p53 restoration in murine liver carcinomas

Wen Xue^{1*}, Lars Zender^{1*}, Cornelius Miething¹, Ross A. Dickins^{1,2}, Eva Hernando³, Valery Krizhanovsky¹, Carlos Cordon-Cardo³, and Scott W. Lowe^{1,2**}

¹ Cold Spring Harbor Laboratory, Cold Spring Harbor, New York 11724, USA

² Howard Hughes Medical Institute, Cold Spring Harbor, NY 11724, USA

³ Division of Molecular Pathology, Memorial Sloan-Kettering Cancer Center, New York 10021, USA

*both authors contributed equally to this work

Supplementary Methods

Generation of liver carcinomas. Isolation, culture and retroviral infection of murine hepatoblasts were described recently^{1,2}. Liver progenitor cells were infected with MSCV retroviruses harboring H-rasV12, a p53 short hairpin RNA driven by the TRE-CMV promoter (TRE.shp53) and tTA. The sequence of the shRNAmir against p53 was 5'-TGCTGTTGACAGTGAGCGCCCACTACAAGTACATGTGTAATAGTGAAGCCACAGATGTATTACACATGTACTTGTAGTGGATGCCTACTGCCTCGA-3' (Color marked sequences denote the mature shRNA, for more information see <http://codex.cshl.edu>). For some experiments the cells were subsequently infected with a luciferase expressing retrovirus and selected with hygromycin. The luciferase-hygro vector was generated by cloning the luciferase cDNA (pGL3, Promega) into a MSCV-Hygro vector (Clontech). Generation of all other vectors has been described recently³. Genetically modified hepatoblasts were introduced into the livers of retrorsine pretreated¹ female NCR nu/nu mice (6-8 weeks of age) by intra-splenic injection. Transplanted cells were allowed to migrate to the recipient liver and

engraft the organ. Tumor progression or regression was monitored by abdominal palpation, whole body GFP imaging and *in vivo* bioluminescence imaging. To generate subcutaneous tumors, female nude mice (NCR nu/nu) mice were γ -irradiated (400 rad) and 3×10^6 cells (unless otherwise noted in the figure legend) were subcutaneously injected into the rear flanks of the mice. Tumor volume (cm^3) was determined by caliper measurement and calculated as $\text{length} \times \text{width}^2 \times \pi / 6$.

Doxycycline (Dox) treatment and *in vivo* bioluminescence imaging. Doxycycline (BD) was refreshed in cell culture medium (100ng/mL) every 2 days. Mice were treated with 0.2mg/mL Dox in 0.5% sucrose solution in light-protected bottles. Dox was refreshed every 4 days. *Bioluminescence* imaging was performed on anaesthetized animals using a Xenogen imager. 200 μ L luciferin salt (Xenogen, 15 mg/mL in PBS) was injected into mice (i.p.) 10-15 minutes before imaging. Exposure time was 30 seconds for animals and 10 seconds for explanted livers.

Histopathology and Immunohistochemistry. Histopathological evaluation of murine liver carcinomas was performed by an experienced pathologist (C.C.C.) using paraffin embedded liver tumor sections stained with Hematoxylin/Eosin. Ki67 and TUNEL staining was performed using standard protocols². Activated caspase 3 (Cell signalling), CK8 (RDI), AFP(Dako), CK7 (Abcam) immunohistochemistry was performed on paraffin embedded liver tumor sections. Positively stained cells were quantified by averaging 3 optical fields (>200 cells per field) under 400X magnification on 4 tumors from 4 individual animals (n=4).

Immunoblotting. Fresh tumor tissue or cell pellets were lysed in Laemmli buffer using a tissue homogenizer. Equal amounts of protein (16 μ g) were separated on 10% SDS-polyacrylamide gels and transferred to PVDF membranes. Blots were probed with antibodies against p53 (Vector Laboratories, IMX25, 1:1000), Ras (Calbiochem, Ab1, 1:1000), Tubulin (B-5-1-2, Sigma; 1:5000),

AFP (Dako; 1:1000), Cytokeratin 8 (RDI, 1:1000), AFP (Dako, 1:1000), Cytokeratin 7 (Abcam, 1:1000), p15 (Cell signaling, 1:1000), p16 (Santa Cruz, M156, 1:500) and DcR2 (Stressgen, 1:2000).

Flow cytometry. Spleen and PB cells were prepared as described recently⁴. Fresh tumor tissues were minced and digested in DMEM containing 1000 U/ml dispase (Invitrogen) at 37°C for 40 minutes. After filtering through a 100µm nylon mesh, the cells were stained with indicated combinations of FITC, PE and APC labeled antibodies (all from BD Pharmingen), counterstained with DAPI to exclude dead cells and analyzed on a BD LSRII flow cytometer.

RNA expression analyses. Murine hepatoma cells or tumors were freshly homogenized in Trizol (GIBCO). RNA was isolated according to the manufacturer's instructions, treated with RNase-free DNase (QIAGEN) and purified with QIAGEN RNAeasy columns. Total RNA was converted to cDNA using TaqMan reverse transcription reagents (Applied Biosystems) and used in qPCR reactions with incorporation of SYBR Green PCR Master Mix (Applied Biosystems). Each reaction was done in triplicate using gene-specific primers. The expression level of each gene was first normalized to *AcRPO* (acidic ribosomal protein P0) and then to the first sample (p53 off) among the tumors or the cells. Similar results were obtained using β -actin as reference gene. Microarray experiments were performed on Mouse Genome 430A 2.0 Arrays (Affymetrix). siRNA northern blotting has been described recently³.

Immunofluorescence and suppression of immune cell function in vivo. Sections (10µm) of snap frozen tumor tissue were fixed with 4% PFA for 10 minutes and subjected to standard immunofluorescence staining using α -Neutrophil (Abcam, NIMP-R14, 1:100) or α -Macrophage (Serotec, CD68 Clone FA-11, 1:100) or α -NK1.1 (BD Pharmingen, 1:100) antibodies together with

DAPI counterstaining. Suppression of macrophage function by GdCl₃ and NK cell function by inhibitory antibody (Wako, Anti asialo GM1) was performed as described recently⁵. GdCl₃ was injected i.v. at 10mg/kg in 200ul saline on Day 0, 1, 4, 8 and 12 after the start of Dox treatment. Anti-NK antibody (GM1) was applied i.v. at 25ul in 200ul saline on the same schedule. The neutrophil inhibitory antibody⁶ (LY-6G, eBioscience) was injected i.p. (150µg in 300µl saline) at d0, d3, d6, d9. Samples for flow cytometry were collected on Day 6 (48hrs after GdCl₃/GM1 treatment and 72 hrs after LY-6G treatment).

Tissue culture and SA-β-Gal assays. Tissue culture, cell counting and colony formation assays were performed as previously described³. 5,000 cells were plated in 10 cm plates for colony formation assay and stained 8 days or 16 days later. Detection of SA-β-gal activity was performed as described before at pH=5.5⁷. Sections (10µm) of snap frozen tumor tissue were fixed with 1% formalin for 1 minute and stained for 12-16hrs. Tumor bearing livers were fixed with 4% formalin overnight, washed with PBS and stained for 4hrs. Cultured cells were fixed with 4% formalin for 5 minutes and stained for 10hrs.

Primer Sequences for RT-Q-PCR

Primers for mouse genes used in RT-Q-PCR reactions were as follows:

MCP-1

5'-gtggggcgtaactgcat-3'

5'-caggtccctgtcatgcttct-3'

CSF-1

5'-tgctaggggtggctttagg-3'

5'-caacagcttgctaagtgtctca-3'

IL15

5'-cgtgctctaccttgcaaaca-3'

5'-tctcctccagctcctcacat-3'

CXCL1

5'-tgttgtgcgaaaagaagtgc-3'

5'-tacaaacacagcctcccaca-3'

VEGFa

5'-ggttcccgaaccctgag-3'

5'-gcagcttgagttaaacaacgacg-3'

AcRP0

5'-ttatcagctgcacatcactcag-3'

5'-cgagaagacctcctttcca-3'

ICAM1

5'-cttccagctaccatcccaaa-3'

5'-cttcagaggcaggaaacagg-3'

β -actin

5'-ccaccgatccacacagagta-3'

5'-ggctcctagcaccatgaaga-3'

Supplementary References

Reference List

1. Zender,L. *et al.* Generation and analysis of genetically defined liver carcinomas derived from bipotential liver progenitors. *Cold Spring Harb. Symp. Quant. Biol.* **70**, 251-261 (2005).
2. Zender,L. *et al.* Identification and validation of oncogenes in liver cancer using an integrative oncogenomic approach. *Cell* **125**, 1253-1267 (2006).
3. Dickins,R.A. *et al.* Probing tumor phenotypes using stable and regulated synthetic microRNA precursors. *Nat. Genet.* **37**, 1289-1295 (2005).
4. Grundler,R., Miething,C., Thiede,C., Peschel,C. & Duyster,J. FLT3-ITD and tyrosine kinase domain mutants induce 2 distinct phenotypes in a murine bone marrow transplantation model. *Blood* **105**, 4792-4799 (2005).
5. Mundt,B. *et al.* Involvement of TRAIL and its receptors in viral hepatitis. *FASEB J.* **17**, 94-96 (2003).
6. Hong,F. *et al.* Beta-glucan functions as an adjuvant for monoclonal antibody immunotherapy by recruiting tumoricidal granulocytes as killer cells. *Cancer Res.* **63**, 9023-9031 (2003).
7. Narita,M. *et al.* Rb-mediated heterochromatin formation and silencing of E2F target genes during cellular senescence. *Cell* **113**, 703-716 (2003).
8. Shultz,L.D. *et al.* Multiple defects in innate and adaptive immunologic function in NOD/LtSz-scid mice. *J. Immunol.* **154**, 180-191 (1995).

Supplementary figure legends

Figure S1 | Regulating p53 expression in liver tumors using conditional RNAi.

a, Retroviral vector maps. **b**, Doxycycline treatment turns off the conditional miR30-based p53 shRNA. Liver tumors co-expressing *ras* and the tet-off p53 shRNA were treated with Dox for the indicated number of days and harvested for Northern blot analysis. Probes were designed against the mature p53 shRNA. U6 RNA was used as a loading control. **c**, Restoration of p53 expression by Dox treatment. Protein lysates from cultured liver progenitor cells expressing *ras* and Tet-off p53 shRNA were immunoblotted for p53, Ras and Tubulin (as a loading control).

Figure S2 | Brief reactivation of p53 results in tumor remission. a, Brief reactivation of p53 is sufficient to suppress colony formation. Liver progenitor cells harboring *ras* and tet-off p53 were plated at low density and either left untreated (p53 off), pulse treated with Dox for 2 or 4 days, or left constantly on Dox (p53 on). Crystal violet staining was performed 8 and 16 days after plating. **b**, Brief reactivation of p53 is sufficient to regress subcutaneous tumors. Nude mice (n=4 for each group) injected with progenitor cells as in **a** were either left untreated (p53 off, upper left), constantly treated with Dox (p53 on, upper right) or briefly treated for 2 (lower left) or 4 (lower right) days. Tumor size was followed up by luciferase imaging. D0 was the initial day of Dox treatment.

Figure S3 | p53 reactivation is associated with cellular differentiation. a, IHC staining of liver tumors for markers of cellular differentiation. Alpha-fetoprotein (AFP) is an embryonic liver- and liver tumor marker, Cytokeratin 8 (CK8) and Cytokeratin 7 (CK7) are hepatocyte and cholangiocyte markers, respectively. Inset denotes CK7 positive bile duct cells. Scale bar, 100µm. **b**,

Immunoblots of cellular differentiation markers in the liver tumors after 0, 4 and 6 days of Dox treatment. Protein lysate from wild type mouse liver was loaded as a control. “*” denotes a non-specific band.

Figure S4 | p53 induced liver tumor regression is associated with infiltration of immune cells. **a**, Histopathological analysis of tumor sections reveals infiltrating immune cells (dashed circle) following p53 reactivation. **b**, High magnification view of representative “p53 on” tumor sections shows granulocyte nuclei (black arrows) and tumor cell nuclei (red arrows). Dashed line denotes the border of the immune cell cluster. As miR30 design shRNA is a physiological trigger of the RNAi machinery and inflammation was only observed after silencing of the p53 shRNA it is unlikely that dsRNAs are involved in triggering the immune response.

Figure S5 | Innate immune cells are infiltrating senescent tumors. Immunofluorescence (IF) staining of tumor cryosections using neutrophil marker NIMP-R14, macrophage marker CD68 or NK cell marker NK1.1. Representative stainings from 2 tumors in each group are shown. Arrowheads indicate positively stained cells in the “p53 on” tumors. Insets denote the high magnification view.

Figure S6 | Immunophenotyping of immune cell population in the senescent tumors. **a**, Quantification of infiltrating immune cells. Single cell suspension from tumors were stained and analyzed by flow cytometry. Viable cells (DAPI⁻) were gated for pan-leukocyte marker CD45-APC. CD45⁺ population was then sub-gated for PE-stained CD11b (myeloid), F4/80 (macrophage), Gr-1

(granulocyte) and CD49b (pan-NK) markers. EGFP was used to distinguish immune cells (GFP⁻) from nonspecific stained tumor cells (GFP⁺). Fold denotes the ratio of leukocyte counts in “p53 on” versus “p53 off” tumors. Shown are the data from a representative experiment (n=2 mice). Error bars indicate s.d. Experiment was repeated two more times using nearby time points (n=2 each) with comparable results. **b**, representative flow cytometry results. Dashed circle in the FSC/SSC dot plot denotes increased granulocyte numbers in the “p53 on” tumors.

Figure S7 | p53-induced tumor regression is accompanied by progressive damage of neo-vasculature. **a**, H&E staining of a Dox untreated liver tumor (p53 off) shows normal blood vessel structure. **b-e**, Dox treated tumors (p53 on) show progressive blood vessel damage in the time course after p53 reactivation. The regressing tumors show perivascular infiltration of immune cells, characterized by ‘plumbed’ (enlarged) endothelial cells and distorted lumens, damaging mainly mid-size blood vessels. By day 8 and more obvious at day 13, an overt vasculitis was observed, producing sclerosed vessels, hemorrhagia and erythrophagocytosis.

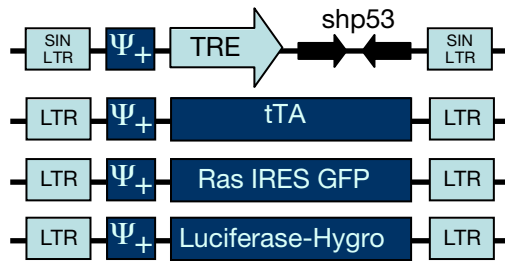
Figure S8 | Efficacy of immune antagonists on depleting the innate immune cells. Spleen cells or peripheral blood (PB) from animals (n=2 for each group) treated with immune antagonists were double stained with the indicated antibodies and analyzed by flow cytometry to quantify the subtypes of innate immune cells (CD11b⁺/Gr1⁺, granulocytes; CD11b⁺/F4/80⁺, macrophages; CD11b⁺/CD49b⁺, NK cells). Circles delineate the depleted populations. The bar graphs (insets) denote the fold change of the indicated leukocyte fraction, with the control set as single fold. The four bars represent the analyzed groups (in the order of control, neutrophil-depleted,

macrophage-depleted, NK cell-depleted), the bar corresponding to the respective dot plot is shown in white. Error bars indicate s.d. (n=2). F4/80 staining of spleen cells revealed some unspecific binding and was therefore not included in the analysis. Depletion of the macrophage/monocyte population by GdCl was also revealed by a reduction of CD11b⁺/Gr-1⁻ cells in the PB of GdCl-treated animals (red arrow).

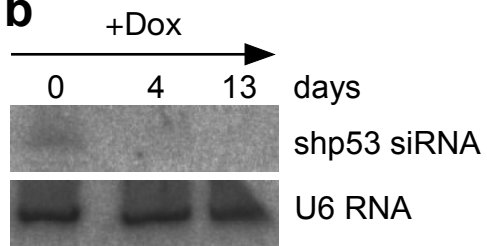
Figure S9 | Defective tumor regression following p53 reactivation in tumors grown in NOD/SCID mice. **a**, Tumors derived from *ras* transformed liver progenitor cells with tet-off shp53 were grown subcutaneously in NCR nu/nu mice (defective in B and T cells, see www.taconic.com) and NOD/SCID mice (defective in B/T cells, and severely impaired in the innate immune system⁸, also see <http://jaxmice.jax.org/library/notes/476b.html>). Values represent mean ± s.d. (n=2). **b**, SA-β-Gal staining of cryosections derived from tumors grown in NOD/SCID mice that were otherwise untreated (top, p53 off) or following 24 days of Dox (bottom, p53 on). Although the tumors do not regress in response to p53 activation, the cells remain viable (see also, c) and undergo senescence. **c**, H&E staining of tumors harboring the conditional p53 shRNA grown in nude mice (nu/nu) or NOD/SCID mice 24 days after Dox administration (p53 on). Immune cells infiltrate tumors grown in nu/nu mice but not those in NOD/SCID animals. Arrowheads denote immune cells. Circle denotes a region particularly enriched for immune cells.

Figure S1

a



b



c

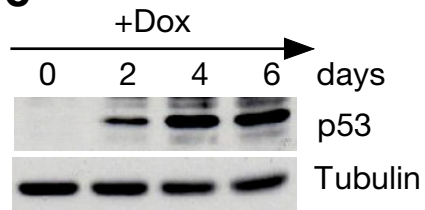


Figure S2

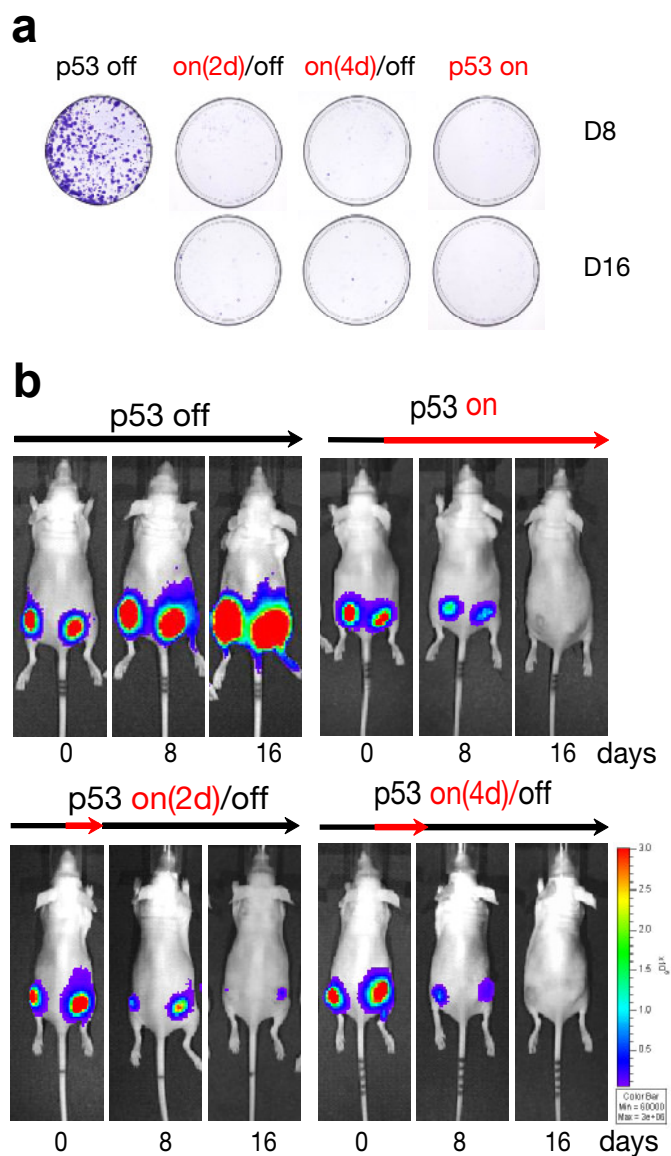


Figure S3

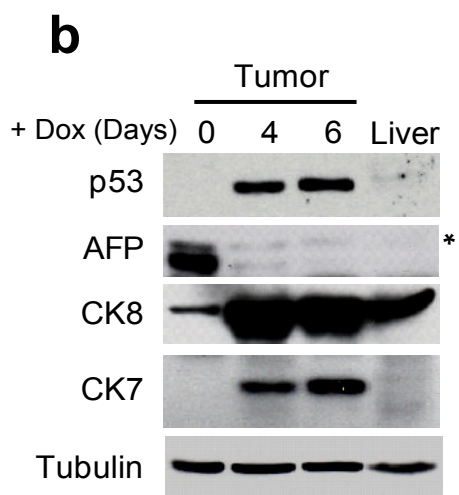
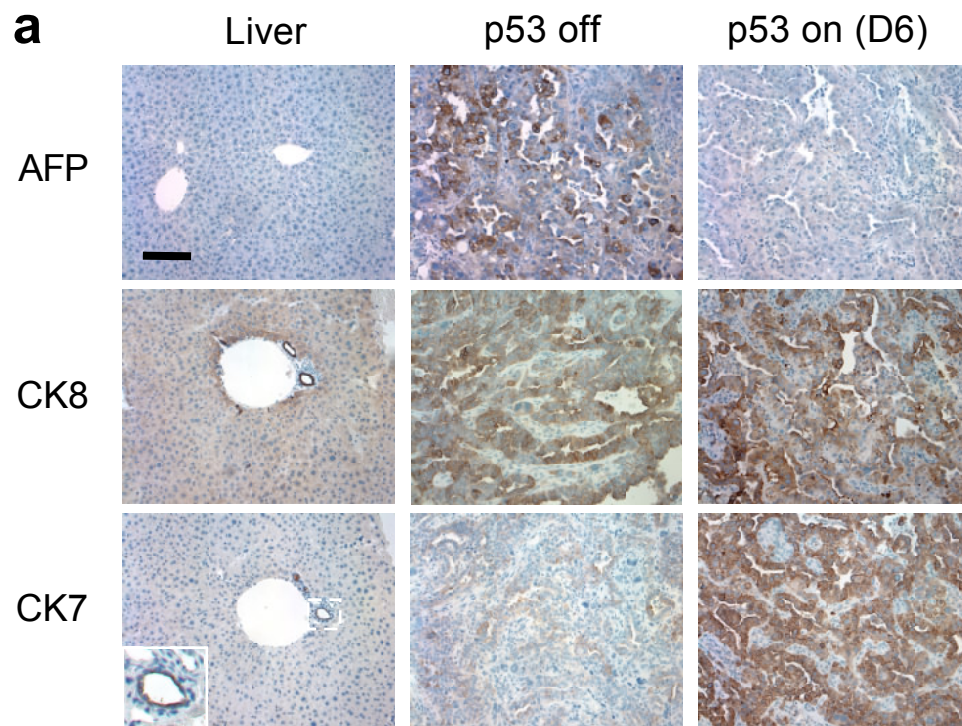


Figure S4

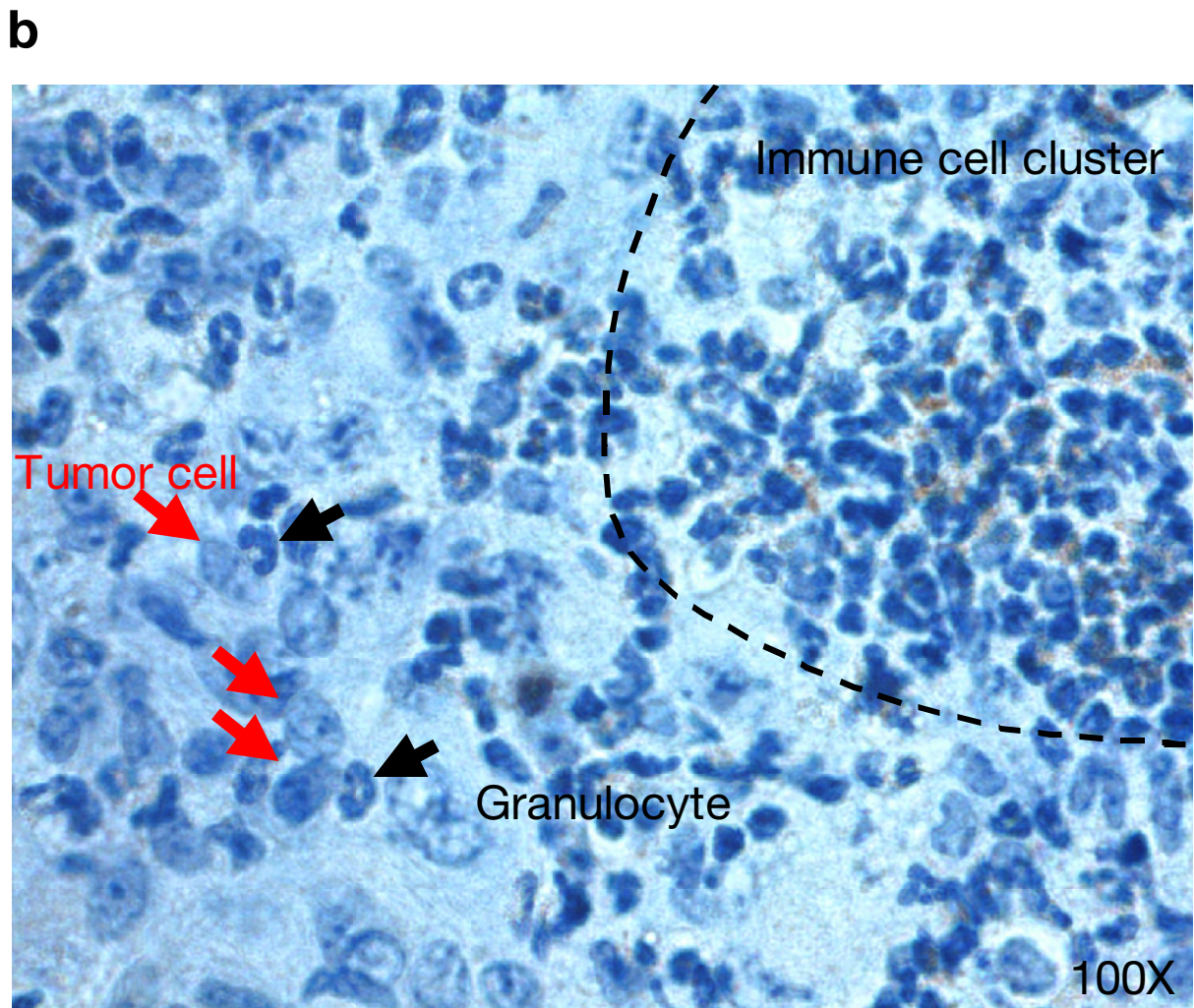
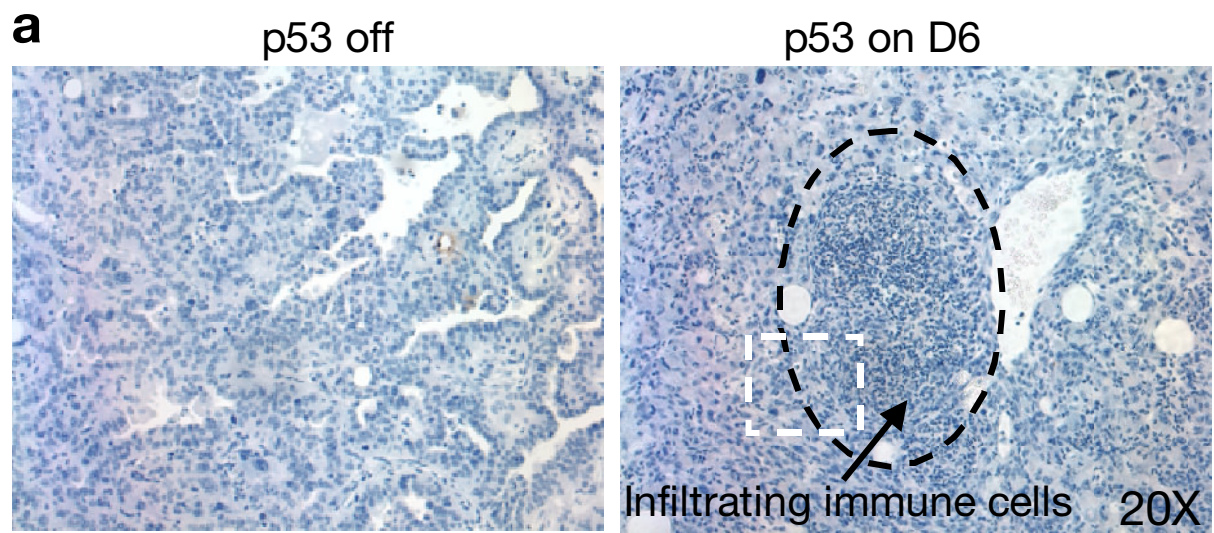
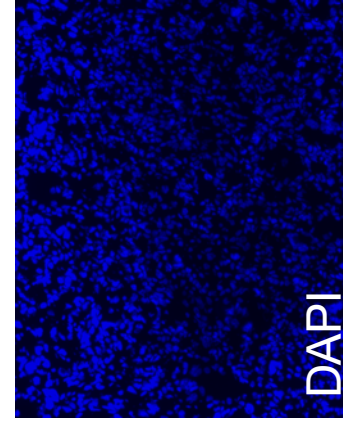
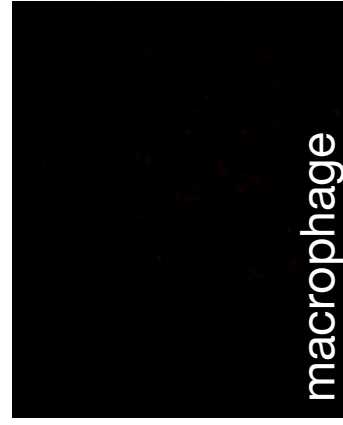
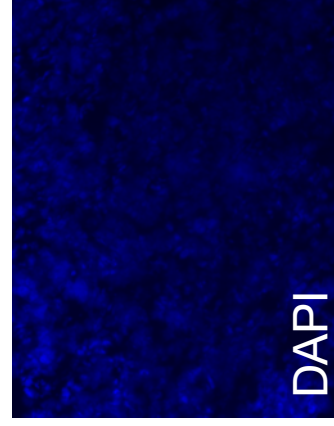
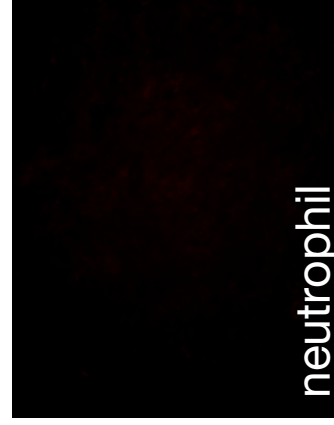


Figure S5.

Tumor (p53 off)



Tumor (p53 on, Day 8)

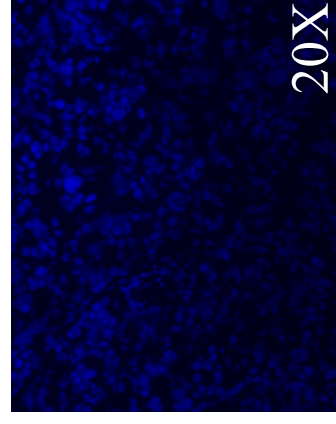
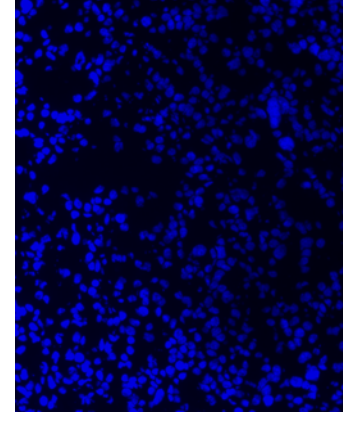
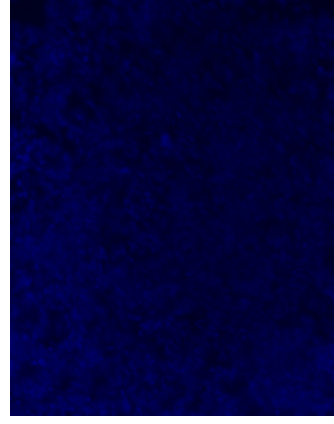
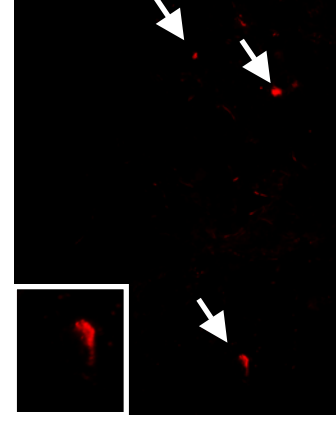
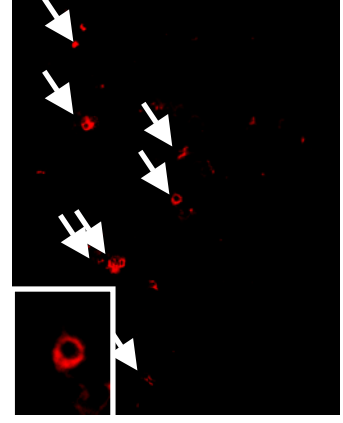
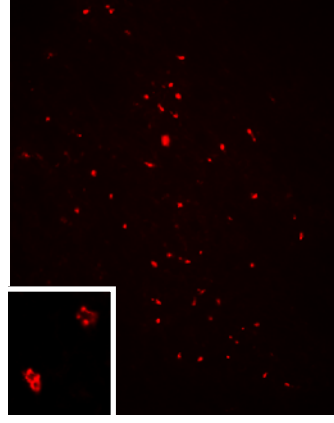


Figure S3.

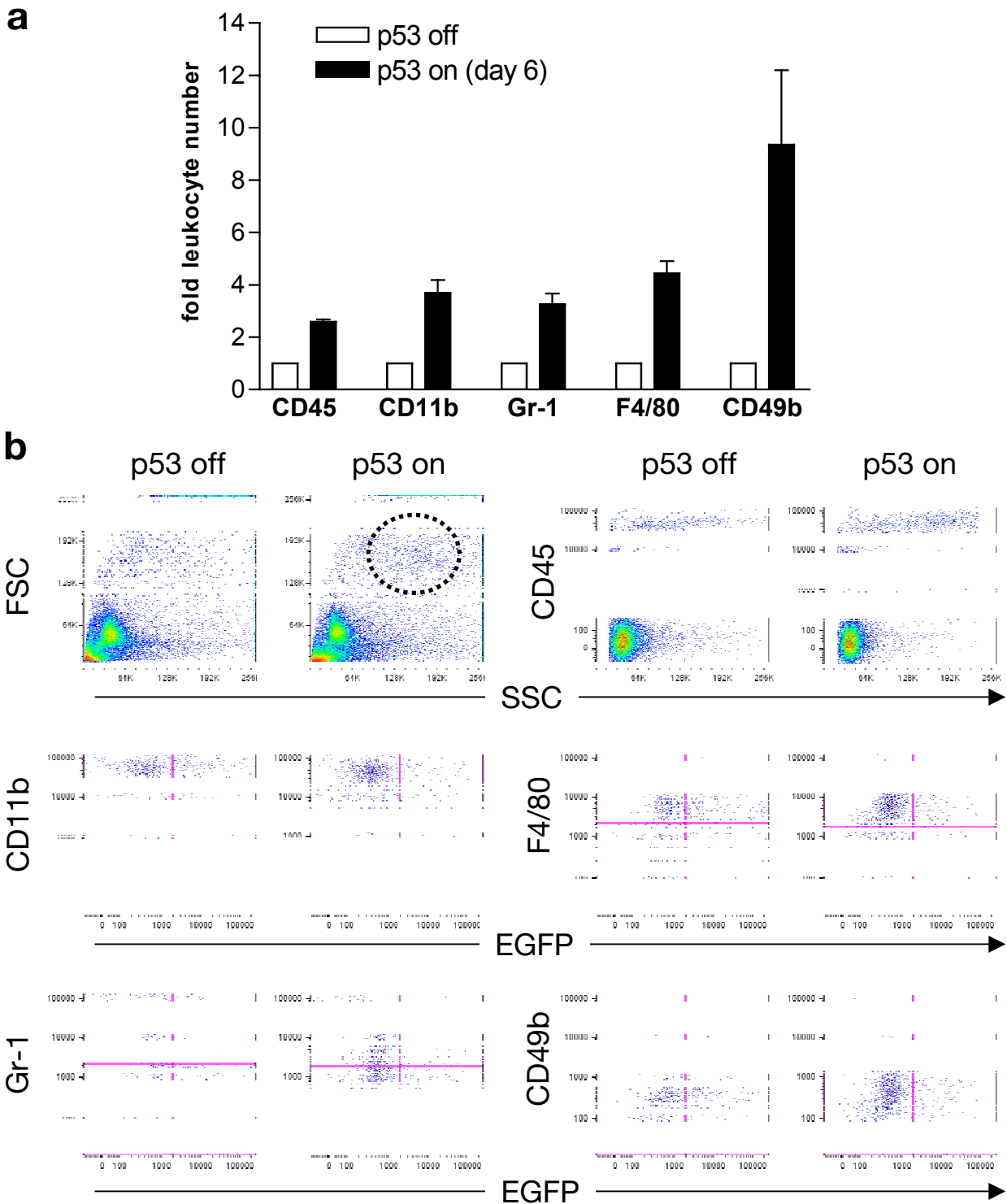
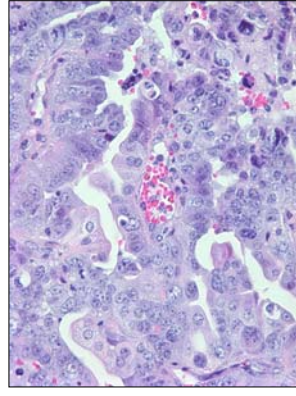


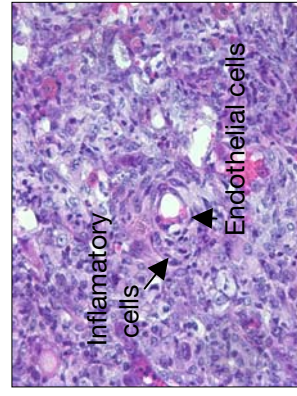
Figure S7.

a p53 off



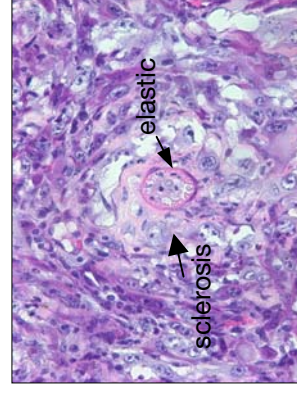
p53 on

b



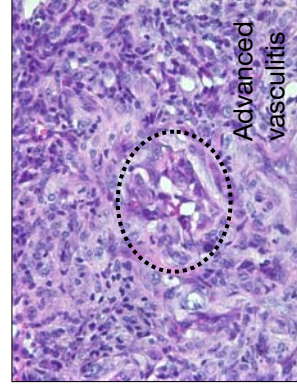
d4

c



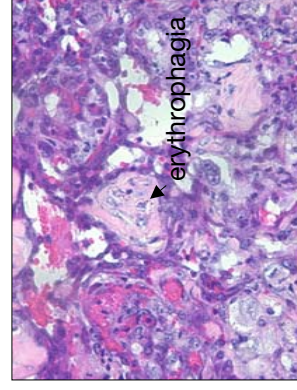
d6

d



d8

e



d13

Figure S9.